

A semi-analytical approach for solving surface motion of multiple alluvial valleys for incident plane SH-waves

Po-Yuan Chen and Jeng-Tzong Chen

Department of Harbor and River Engineering,
National Taiwan Ocean University, Keelung, Taiwan
M93520010@mail.ntou.edu.tw

NSC PROJECT: NSC-95-2115-M-019-003-MY2

ABSTRACT

In this paper, the degenerate kernels and Fourier series expansions are adopted in the null-field integral equation to solve the exterior Helmholtz problems with alluvial valleys. The main gain of using degenerate kernels in integral equations is free of calculating the principal values for singular integrals when the null-field point exactly locates on the real boundary. An adaptive observer system is addressed to fully employ the property of degenerate kernels for circular boundaries in the polar coordinate. Image concept and technique of decomposition are utilized for half-plane problems. After moving the null-field point to the boundary and matching the boundary conditions, a linear algebraic system is obtained without boundary discretization. The unknown coefficients in the algebraic system can be easily determined. The present method is treated as a "semi-analytical" solution since error only attributes to the truncation of Fourier series. Earthquake analysis for the site response of alluvial valley or canyon subject to the incident SH-wave is the main concern. Numerical examples including single and successive alluvial valleys are given to test our program. Limiting cases of a single canyon and two successive canyons are also addressed. The validity of the semi-analytical method is verified. Our advantages, well-posed model, principal value free, elimination of boundary layer effect and exponential convergence and mesh-free, by using the present method are achieved.

Keywords: degenerate kernel, Fourier series, null-field integral equation, Helmholtz problem, SH-wave, alluvial valley.

1. INTRODUCTION

One of the major concerns of engineering seismology is to understand and explain vibrational response of the soil excited by earthquakes. The problem of the scattering and diffraction of SH-waves by a two-dimensional arbitrary number and location of cavities and inclusions in full and half-planes is revisited in this paper by using our unified formulation. In 1971, Trifunac [1] has solved the problem of a single semi-circular alluvial valley subject to SH-wave. Later, Pao and Mao [2] have published a book on the stress

concentration in 1972. In 1973, Trifunac [3] has also derived the closed-form solution of a single semi-circular canyon subject to the SH-wave. The earliest reference to a closed-form solution of the scattering and diffraction of the incident SH-wave by an underground inclusion exists in an article concerning an underground circular tunnel by Lee and Trifunac [4]. In order to extend to arbitrary shape inclusion problems, Lee and Manooch [5] have used the weighted residual method to revisit the problem of scattering and diffraction of SH-wave with respect to an underground cavity of arbitrary shape in a two-dimensional elastic half-plane. In the following years, they extended to the half-plane problem with a inclusion of arbitrary shape [6,7]. According to the literature review, it is observed that exact solutions for boundary value problems are only limited for simple cases, *e.g.* half-plane with a semi-circular canyon, a cavity under half-plane, an inclusion under half-plane. Numerical approach using boundary integral formulation was employed to study diffraction of seismic waves in half-plane [8]. Therefore, proposing a systematic approach for solving exterior Helmholtz problems with circular boundaries of various numbers, positions and radii is our goal in this paper. Our approach can deal with a cavity problem as a limiting case of an inclusion problem with zero shear modulus.

In this paper, the boundary integral equation method (BIEM) is utilized to solve the half-plane radiation and scattering problems with circular boundaries. To fully utilize the geometry of circular boundary after introducing image concept, not only Fourier series for boundary densities as previously used by many researchers but also the degenerate kernel for fundamental solutions in the present formulation is incorporated into the null-field integral equation. The key idea is that we can push the null-field point exactly on the real boundary by using appropriate degenerate kernel in real computation. All the improper boundary integrals are free of calculating the principal values (Cauchy and Hadamard) in place of series sum. In integrating each circular boundary for the null-field equation, the adaptive observer system of polar coordinate is considered to fully employ the property of degenerate kernel. For the hypersingular equation, vector decomposition for the radial and tangential gradients is carefully considered, especially in the nonfocal case. A

scattering problem subject to the incident wave is decomposed into two parts, incident plane wave field and radiation field. The radiation boundary condition is the minus quantity of incident wave function for matching the boundary condition of total wave for a cavity. Therefore, proposing a systematic approach for solving BVP with various numbers of circular boundaries and arbitrary positions and radii is our goal in this paper. Following the success of torsion, bending and anti-plane problems with circular holes [9,10,11,12], the amplification of site response for alluvial valleys is studied.

2. PROBLEM STATEMENT

Half-plane problems with alluvial to be analyzed is shown in Figure 1. The matrix and alluvial are assumed to be elastic, isotropic and homogenous, and the interface between the alluvial and matrix is assumed to be perfect. The governing equation of the anti-plane SH-wave harmonic motion is

$$\mu \nabla^2 w(x) + \rho \omega^2 w(x) = 0, \quad x \in \Omega \quad (1)$$

where μ , ρ and ω are the material properties of shear modulus, the density and the frequency, ∇^2 and Ω are the Laplacian operator and the domain of interest, respectively. The anti-plane displacement field is defined as

$$u = v = 0, \quad w = w(x, y), \quad (2)$$

where w is the only nonvanishing component of displacement with respect to the Cartesian coordinate which is a function of x and y . The traction free boundary condition at the ground surface of the half-plane is defined as follows

$$\tau_{yz} = \mu \frac{\partial w}{\partial y} = 0, \quad y = 0, \quad (3)$$

or can be represented in the polar coordinate as

$$\tau_\theta = \frac{\mu}{r} \frac{\partial w}{\partial \theta} = 0, \quad \theta = 0 \text{ and } \pi. \quad (4)$$

The incident excitation of the half-plane, w^{in} , is defined as a steady-state plane SH-wave, and motion in the z direction. It is expressed as shown below:

$$w^{in} = W_0 e^{ik(x \sin \gamma + y \cos \gamma)}, \quad (5)$$

where W_0 is the constant amplitude, and γ is the angle of incidence.

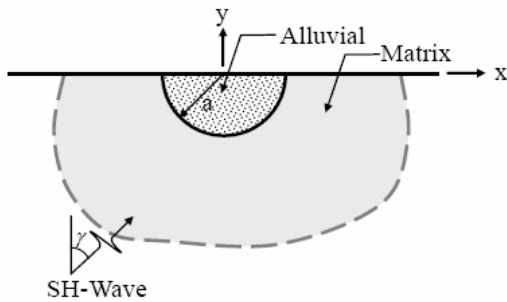


Figure 1 A half-plane problem with a semi-circular alluvial valley subject to the SH-wave.

3. DUAL BOUNDARY INTEGRAL FORMULATION

Regarding to the SH-wave problem, the integral equation for the domain point can be derived from the third Green's identity [13], yields

$$2\pi u(x) = \int_B T^e(s, x) u(s) dB(s) - \int_B U^e(s, x) t(s) dB(s), \quad x \in \Omega \cup B, \quad (6)$$

$$2\pi t(x) = \int_B M^e(s, x) u(s) dB(s) - \int_B L^e(s, x) t(s) dB(s), \quad x \in \Omega \cup B, \quad (7)$$

where the four kernels should be selected in a degenerate form of exterior region with the superscript "e", s and x are the source and field points, respectively, B is the boundary, and the kernel function, $U(s, x)$, is the fundamental solution which satisfies

$$(\nabla^2 + k^2)U(x, s) = 2\pi\delta(x-s), \quad (8)$$

where $\delta(x-s)$ denotes the Dirac-delta function. Then, we can obtain the fundamental solution as follows

$$U(s, x) = \frac{-i\pi H_0^{(1)}(kr)}{2}, \quad (9)$$

$$T(s, x) = \frac{\partial U(s, x)}{\partial n_s}, \quad L(s, x) = \frac{\partial U(s, x)}{\partial n_x}, \quad (10)$$

$$M(s, x) = \frac{\partial^2 U(s, x)}{\partial n_x \partial n_s},$$

where $H_n^{(1)}(kr)$ is the n th order Hankel function of the first kind, $r \equiv |s-x|$, n_x denotes the outward normal vector at the field point x . By collocating x outside the domain ($x \in \Omega^c$) or on the boundary (B), we obtain the dual null-field integral equations as shown below

$$0 = \int_B T^i(s, x) u(s) dB(s) - \int_B U^i(s, x) t(s) dB(s), \quad x \in \Omega^c \cup B, \quad (11)$$

$$0 = \int_B M^i(s, x) u(s) dB(s) - \int_B L^i(s, x) t(s) dB(s), \quad x \in \Omega^c \cup B, \quad (12)$$

where Ω^c is the complementary domain and the four kernels are chosen appropriately using degenerate expression of interior region with the superscript "i" in the following section.

4. EXPANSIONS OF FUNDAMENTAL SOLUTIONS AND BOUNDARY DENSITIES

In the present method, we adopt the mathematical tools, degenerate kernels, for the purpose of analytical study. The combination of degenerate kernels and Fourier series plays the major role in handling problems with circular boundaries. Based on the separable property, the kernel function $U(s, x)$, $T(s, x)$, $L(s, x)$ and

$M(s, x)$ can be expanded into separable form by $(x = (\rho, \phi))$ in the polar coordinate [14].
dividing the source point $(s = (R, \theta))$ and field point

$$U(s, x) = \begin{cases} U^i(s, x) = \frac{-\pi i}{2} \sum_{m=0}^{\infty} \varepsilon_m J_m(k\rho) H_m^{(1)}(kR) \cos(m(\theta - \phi)), R \geq \rho \\ U^e(s, x) = \frac{-\pi i}{2} \sum_{m=0}^{\infty} \varepsilon_m H_m^{(1)}(k\rho) J_m(kR) \cos(m(\theta - \phi)), \rho > R \end{cases}, \quad (13)$$

$$T(s, x) = \begin{cases} T^i(s, x) = \frac{-\pi k i}{2} \sum_{m=0}^{\infty} \varepsilon_m J_m(k\rho) H_m^{(1)}(kR) \cos(m(\theta - \phi)), R > \rho \\ T^e(s, x) = \frac{-\pi k i}{2} \sum_{m=0}^{\infty} \varepsilon_m H_m^{(1)}(k\rho) J_m'(kR) \cos(m(\theta - \phi)), \rho > R \end{cases}, \quad (14)$$

$$L(s, x) = \begin{cases} L^i(s, x) = \frac{-\pi k i}{2} \sum_{m=0}^{\infty} \varepsilon_m J_m'(k\rho) H_m^{(1)}(kR) \cos(m(\theta - \phi)), R > \rho \\ L^e(s, x) = \frac{-\pi k i}{2} \sum_{m=0}^{\infty} \varepsilon_m H_m^{(1)}(k\rho) J_m(kR) \cos(m(\theta - \phi)), \rho > R \end{cases}, \quad (15)$$

$$M(s, x) = \begin{cases} M^i(s, x) = \frac{-\pi k^2 i}{2} \sum_{m=0}^{\infty} \varepsilon_m J_m'(k\rho) H_m^{(1)}(kR) \cos(m(\theta - \phi)), R \geq \rho \\ M^e(s, x) = \frac{-\pi k^2 i}{2} \sum_{m=0}^{\infty} \varepsilon_m H_m^{(1)}(k\rho) J_m'(kR) \cos(m(\theta - \phi)), \rho > R \end{cases}, \quad (16)$$

where $i^2 = -1$, the superscripts “ i ” and “ e ” denote the interior and exterior cases for the expressions of kernel, respectively, and ε_m is the Neumann factor

$$\varepsilon_m = \begin{cases} 1, & m = 0 \\ 2, & m = 1, 2, \dots, \infty \end{cases}. \quad (17)$$

It is noted that the larger argument is imbedded in the complex Hankel function (H) instead of real Bessel function (J) to ensure the $H_0(kr)$ singularity and series convergence. Since the potential resulted from $T(s, x)$ and $L(s, x)$ kernels are discontinuous cross the boundary, the potentials of $T(s, x)$ for $R \rightarrow \rho^+$ and $R \rightarrow \rho^-$ are different. This is the reason why $R = \rho$ is not included in expressional degenerate kernels of $T(s, x)$ and $L(s, x)$ in Eqs. (14) and (15). The analytical evaluation of the integrals for each element in the influence matrix can be found [9] and they are all non-singular. Besides, the limiting case to the boundary is also addressed. The continuous and jump behavior across the boundary is well described by using the Wronskian property of J_m and Y_m

$$\begin{aligned} W(J_m(kR), Y_m(kR)) \\ = Y_m'(kR) J_m(kR) - Y_m(kR) J_m'(kR), \\ = \frac{2}{\pi k R} \end{aligned} \quad (18)$$

to display the jump behavior as shown below:

$$\begin{aligned} \int_0^{2\pi} (T^i(s, x) - T^e(s, x)) \cos(n\theta) R d\theta \\ = kR\pi^2 J_n(kR) [Y_n'(kR) - iJ_n'(kR)] \cos(n\phi), \\ -kR\pi^2 J_n'(kR) [Y_n(kR) - iJ_n(kR)] \cos(n\phi) \\ = 2\pi \cos(n\phi) \end{aligned} \quad (19)$$

$$\begin{aligned} \int_0^{2\pi} (T^i(s, x) - T^e(s, x)) \sin(n\theta) R d\theta \\ = kR\pi^2 J_n(kR) [Y_n'(kR) - iJ_n'(kR)] \sin(n\phi) \\ -kR\pi^2 J_n'(kR) [Y_n(kR) - iJ_n(kR)] \sin(n\phi) \\ = 2\pi \sin(n\phi) \end{aligned} \quad (20)$$

The two functions, J and Y , are similar to the two bases, 1 and x , for 1-D rod case where their Wronskian can describe the jump behavior.

Since only circular boundary is considered in this study, we employ the Fourier series expansions to approximate the potential u and its normal derivative t on the circular boundary, we have

$$\begin{aligned} u(s_k) = a_0^k + \sum_{n=1}^{\infty} (a_n^k \cos n\theta_k + b_n^k \sin n\theta_k), \\ s_k \in B_k, \quad k = 1, 2, \dots, N, \end{aligned} \quad (21)$$

$$\begin{aligned} t(s_k) = p_0^k + \sum_{n=1}^{\infty} (p_n^k \cos n\theta_k + q_n^k \sin n\theta_k), \\ s_k \in B_k, \quad k = 1, 2, \dots, N, \end{aligned} \quad (22)$$

where $t(s_k) = \partial u(s_k) / \partial n_s$ in which n_s denotes the outward normal vector at the source point s , a_n^k , b_n^k , p_n^k and q_n^k ($n = 0, 1, 2, \dots$) are the Fourier coefficients and θ_k is the polar angle for the k th circular boundary.

5. ADAPTIVE OBSERVER SYSTEM

Consider a boundary value problem with circular boundaries of arbitrary locations as shown in Figure 2. The rule of objectivity is obeyed since the boundary integral equations are frame indifferent. An adaptive observer system is addressed to fully employ the property of degenerate kernels for circular boundaries in the polar coordinate as shown in Figures 3 (a) and (b). For the integration, the origin of the observer system can be

adaptively located on the center of the corresponding boundary contour. The dummy variable in the circular boundary integration is the angle (θ) instead of radial coordinate (R). By using the adaptive system, all the integrations can be easily calculated.

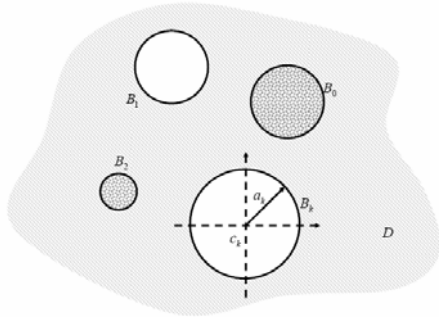


Figure 2 Problem statement

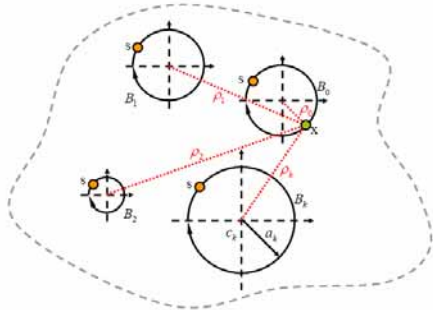


Figure 3 (a) Sketch of the null-field integral equation in conjunction with the adaptive observer system

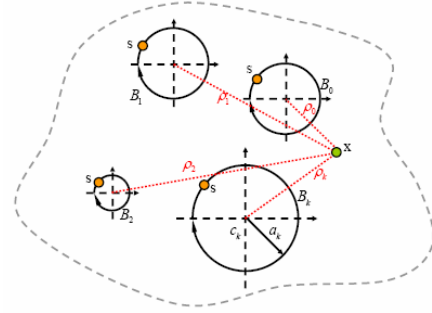


Figure 3 (b) Sketch of the boundary integral equation for the domain point in conjunction with the adaptive observer system.

6. IMAGE TECHNIQUE FOR SOLVING HALF-PLANE SCATTERING PROBLEM

Image concept for half-plane problems

For the half-plane problem with an alluvial valley as shown in Figure 4, we extend the problem into a full plane with the scatter by using image concept such that our formulation can be applied. By applying the concept of even function, the symmetry condition is utilized to satisfy the traction free ($t = 0$) condition on the ground surface. We merge the half-plane domain into the full-plane problem by adding with the reflective wave. To solve the problem, the decomposition technique is employed by introducing two plane waves, one is incident and the other is reflective, instead of only one incident wave. After taking the free body of full-plane problem through the ground surface, we obtain the desired solution which satisfies the Helmholtz equation and all the boundary conditions in the half-plane domain.

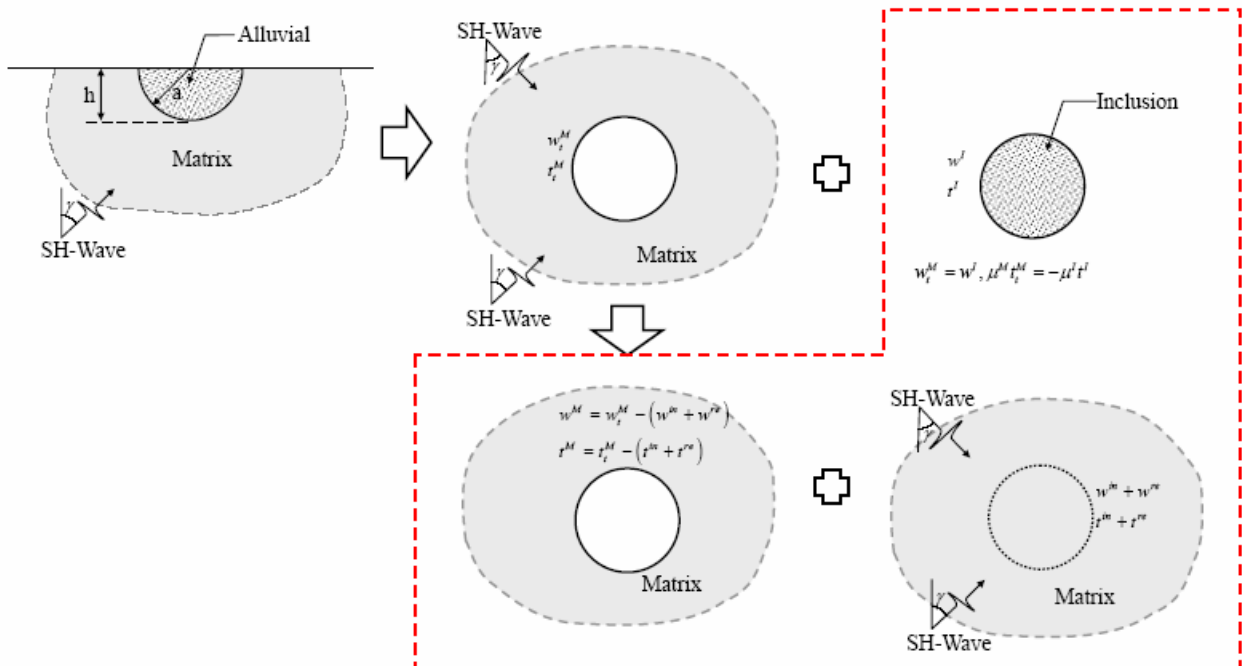


Figure 4 Image concept and the decomposition of superposition of an alluvial valley

Decomposition of scattering problem into incident wave field and radiation problems

For the scattering problem subject to the incident

wave, this problem can be decomposed into two parts. One is the incident wave field and another is the radiation field as shown in Figure 4. The relations between two

parts are shown below:

$$\mathbf{u}_i^M = \mathbf{u}^{in} + \mathbf{u}^{re} + \mathbf{u}^M, \quad (34)$$

$$\mathbf{t}_i^M = \mathbf{t}^{in} + \mathbf{t}^{re} + \mathbf{t}^M, \quad (35)$$

where the “ \mathbf{t}_i^M ” denotes the total field of matrix including radiation and scattering. The subscripts “in” and “re” are the incident and reflected waves and the “ \mathbf{t}^M ” denotes the radiation part of matrix and needs to be solved. To match the boundary condition for the cavity case, the total traction is defined as $\mathbf{t}_i^M = 0$. For the inclusion case, we have the two constraints of the continuity of displacement and equilibrium of traction along the k th interface ($B_k, k = 1, \dots, N$) as shown below:

$$\mathbf{u}_i^M = \mathbf{u}^I \text{ on } B_k, \quad (36)$$

$$\mu^M \mathbf{t}_i^M = -\mu^I \mathbf{t}^I \text{ on } B_k. \quad (37)$$

The radiation parts of matrix (\mathbf{u}^M and \mathbf{t}^M) and inclusion (\mathbf{u}^I and \mathbf{t}^I) can be solved by employing our method.

7. LINEAR ALGEBRAIC SYSTEM AND MATCHING OF INTERFACE CONDITIONS FOR PROBLEMS OF INCLUSION

According to the linear algebraic system, the two systems of matrix and inclusion yield

$$[\mathbf{U}^M] \{ \mathbf{t}^M \} = [\mathbf{T}^M] \{ \mathbf{u}^M \}, \quad (38)$$

$$[\mathbf{U}^I] \{ \mathbf{t}^I \} = [\mathbf{T}^I] \{ \mathbf{u}^I \}. \quad (39)$$

By employing the image concept, the decomposition and superposition, the Eq. (38) can be rewritten as

$$[\mathbf{U}^M] \{ \mathbf{t}_i^M - \mathbf{t}^{in+re} \} = [\mathbf{T}^M] \{ \mathbf{u}_i^M - \mathbf{u}^{in+re} \}. \quad (40)$$

According to Figure 4, an alluvial valley problem can be extended to a full-plane problem with a circular inclusion. In order to satisfy the traction free condition on the surface, the reflective wave is chosen to satisfy the symmetry condition as

$$w^{re} = W_0 e^{ik(x \sin \gamma - y \cos \gamma)}, \quad (41)$$

and we have the two constraints of the continuity of displacement and equilibrium of traction along the j th interface (B_j). We will employ the two constraints into the formulation as shown below:

$$\{ \mathbf{u}_i^M \} = \{ \mathbf{u}^I \} \text{ on } B_k, \quad (42)$$

$$[\boldsymbol{\mu}^M] \{ \mathbf{t}_i^M \} = -[\boldsymbol{\mu}^I] \{ \mathbf{t}^I \} \text{ on } B_k, \quad (43)$$

where $[\boldsymbol{\mu}^M]$ and $[\boldsymbol{\mu}^I]$ can be defined as follows:

$$[\boldsymbol{\mu}^M] = \begin{bmatrix} \mu^M & 0 & \cdots & 0 \\ 0 & \mu^M & \cdots & 0 \\ \vdots & \vdots & \ddots & \vdots \\ 0 & 0 & \cdots & \mu^M \end{bmatrix}, [\boldsymbol{\mu}^I] = \begin{bmatrix} \mu^I & 0 & \cdots & 0 \\ 0 & \mu^I & \cdots & 0 \\ \vdots & \vdots & \ddots & \vdots \\ 0 & 0 & \cdots & \mu^I \end{bmatrix}, \quad (44)$$

where μ^M and μ^I denote the shear modulus of the matrix and the k th inclusion, respectively. By

assembling the matrices in Eqs. (39), (40), (42) and (43), we have

$$\begin{bmatrix} \mathbf{T}^M & -\mathbf{U}^M & \mathbf{0} & \mathbf{0} \\ \mathbf{0} & \mathbf{0} & \mathbf{T}^I & -\mathbf{U}^I \\ \mathbf{I} & \mathbf{0} & -\mathbf{I} & \mathbf{0} \\ \mathbf{0} & \boldsymbol{\mu}^M & \mathbf{0} & \boldsymbol{\mu}^I \end{bmatrix} \begin{Bmatrix} \mathbf{u}_i^M \\ \mathbf{t}_i^M \\ \mathbf{u}^I \\ \mathbf{t}^I \end{Bmatrix} = \begin{Bmatrix} \mathbf{u}(\mathbf{x})^{in+re} \\ \mathbf{0} \\ \mathbf{0} \\ \mathbf{0} \end{Bmatrix}, \quad (45)$$

where $[\mathbf{I}]$ is the identity matrix, and $\{ \mathbf{u}(\mathbf{x})^{in+re} \}$ is shown below

$$\{ \mathbf{u}(\mathbf{x})^{in+re} \} = \langle \mathbf{T}^M \quad -\mathbf{U}^M \rangle \begin{Bmatrix} \mathbf{u}^{in} + \mathbf{u}^{re} \\ \mathbf{t}^{in} + \mathbf{t}^{re} \end{Bmatrix}. \quad (46)$$

The analytical integrals for each element in the influence matrix are all non-singular. Besides, the limiting behavior to the boundary also exist. The direction of contour integration should be taken care, *i.e.*, counterclockwise and clockwise directions are for the interior and exterior problems, respectively. By rearranging the known and unknown sets, the Fourier coefficients can be obtained. After obtaining the unknown Fourier coefficients, the origin of observer system is set to c_j in the B_j integration as shown in Figure 3 (b) to obtain the potential by employing Eq. (6).

8. CALCULATION OF SURFACE DISPLACEMENT

In order to check the validity of the formulation, the Manoogian [6] and Trifunac's [1] problem with an alluvial valley is revisited. We follow the same parameter, η , for comparison purpose. The dimensionless frequency η is defined as shown below:

$$\eta = \frac{2a}{\lambda} = \frac{k^M a}{\pi} = \frac{\omega a}{\pi c^M}, \quad (47)$$

where a is the half-width of the alluvial valley, ω is the angular frequency, k^M and c^M are the shear wave number and the velocity of shear wave for the matrix medium, respectively, and the shear wave number k is defined as

$$k = \frac{\omega}{c}. \quad (48)$$

Substituting Eq. (47) into Eq. (48), the wave number of matrix field is rewritten as

$$k^M = \frac{\pi \eta}{a}, \quad (49)$$

and the shear wave number for the inclusion field is obtained by

$$\frac{k^I}{k^M} = \frac{c^M}{c^I} = \left(\frac{\mu^M}{\mu^I} \cdot \frac{\rho^I}{\rho^M} \right)^{1/2}. \quad (50)$$

Equation (50) indicates that various mediums yield different wave numbers. The surface amplitude is an important index for the earthquake engineering. If the amplitude of incident plane SH-wave is one, the responses at different locations represent amplifications of the incident wave. The resultant motion is defined by the modulus

$$Amplitude = \sqrt{\text{Re}^2(w) + \text{Im}^2(w)}, \quad (51)$$

where $\text{Re}(w)$ and $\text{Im}(w)$ are the real and imaginary parts of total displacement, respectively.

9. ILLUSTRATIVE EXAMPLES AND DISCUSSIONS

In the section, we revisit the same problems of Manoogian and Lee [7], Trifunac [1] and Tsaur *et al.* [15] for the alluvial problem. In order to check the accuracy of the present method, the limiting case is conducted. All the numerical results are given below by using ten terms of Fourier series.

Case 1: Half-plane problem with an alluvial valley subject to the SH-wave

In the following examples, we choose the same parameters $h/a = 1.5$, $\mu^I / \mu^M = 1/6$ and $\rho^I / \rho^M = 2/3$ which were previously adopted in the Ph. D dissertation of Manoogian [6], and four various incident angles ($\gamma = 0^\circ, 30^\circ, 60^\circ$ and 90°) are

considered. The figures show the displacement amplitude on the ground surface only. Displacements are plotted with respect to the dimensionless distance x/a for a specified parameter $\eta = 2$. In order to verify the limiting case of the general program, we set $\mu^I / \mu^M = 10^{-8}$ to reduce to the canyon cases. In Figures 5 and 6, good agreements are obtained after comparing with Lee and Manoogian's results [16] using various frequency parameters of η for the alluvial valley and semi-circular canyon case.

Another limiting case of the rigid alluvial is also of interest in the foundation engineering. For example, rigid footing is a popular model in geotechnical engineering. By setting μ^I / μ^M to be infinity, the limiting case of rigid inclusion can be obtained. Figure 7 plots the surface displacement by setting $\mu^I / \mu^M = 10^4$ and $\eta = 2$ in the real computation. In the range of $x/a = -1$ to 1, the amplification is a constant as expected, because it is undeformed due to the rigid alluvial.

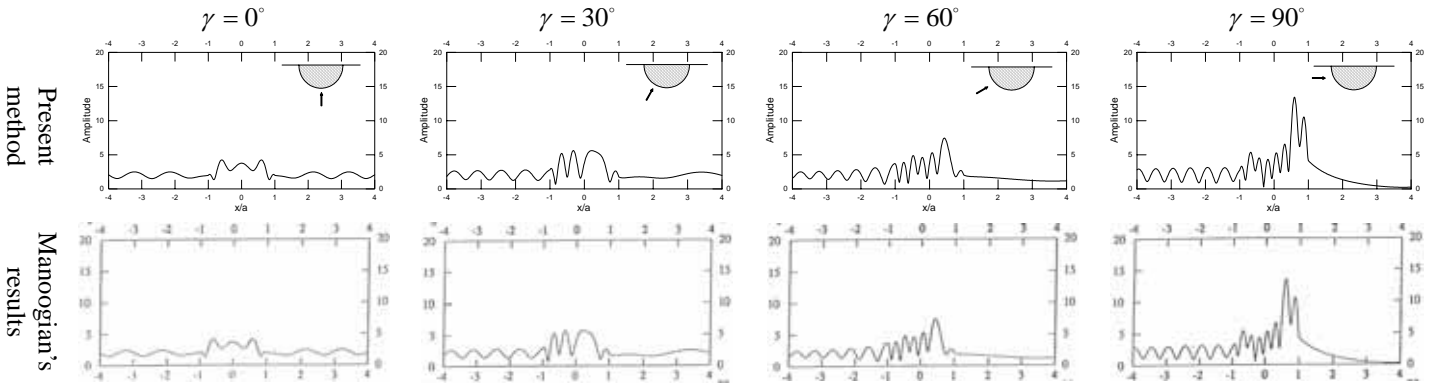


Figure 5 Surface amplitudes of the alluvial valley problem for $\eta = 2.0$ ($\mu^I / \mu^M = 1/6, \rho^I / \rho^M = 2/3$).

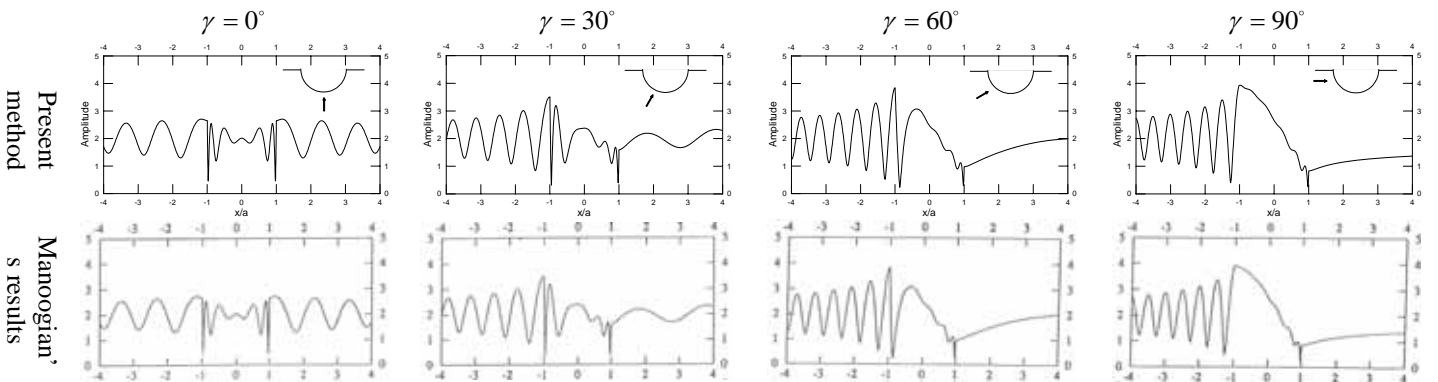


Figure 6 Limiting case of a canyon ($\rho^I / \rho^M = 2/3, \mu^I / \mu^M = 10^{-8}$ and $\eta = 2$).

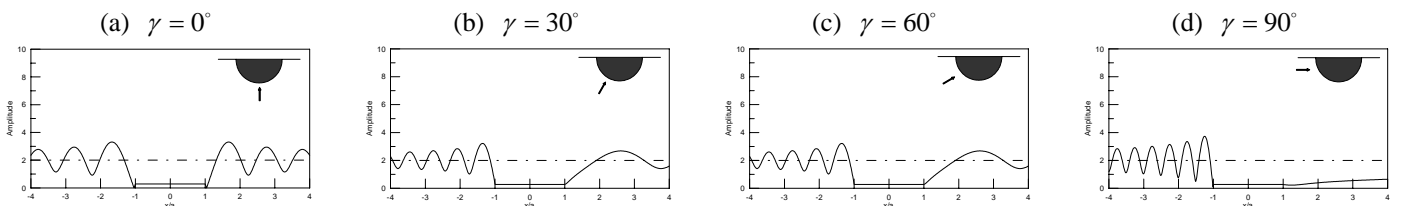


Figure 7 Limiting case of a rigid alluvial valley ($\mu^I / \mu^M = 10^4, \rho^I / \rho^M = 2/3$ and $\eta = 2$).

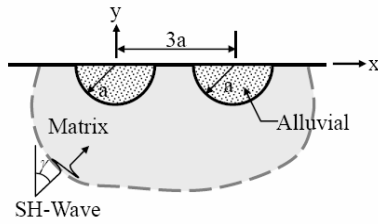


Figure 8 A half-plane problem with two alluvial valleys subject to the incident SH-wave.

Case 2: Half-plane problem with two alluvial valleys subject to the SH-wave

Two semi-circular alluvial valleys subject to the incident SH-wave of γ angle are shown in Figure 8. Figure 9 shows the surface displacements versus x/a for various incident angles with $\mu^I / \mu^M = 1/6$ and $\rho^I / \rho^M = 2/3$ subject to the cases of $\eta = 2$. By setting

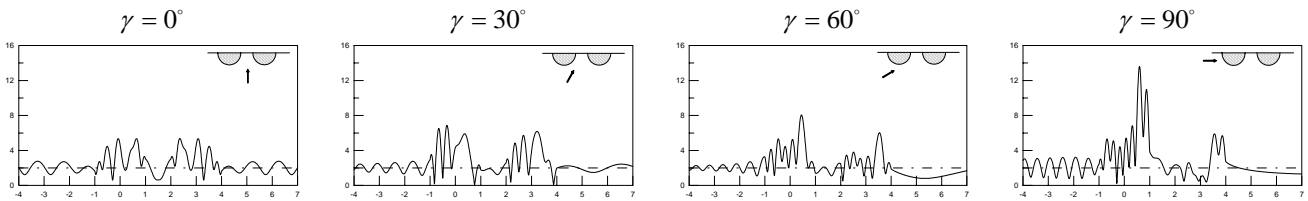


Figure 9 Surface displacements of two alluvial valleys ($\mu^I / \mu^M = 1/6$, $\rho^I / \rho^M = 2/3$ and $\eta = 2$).

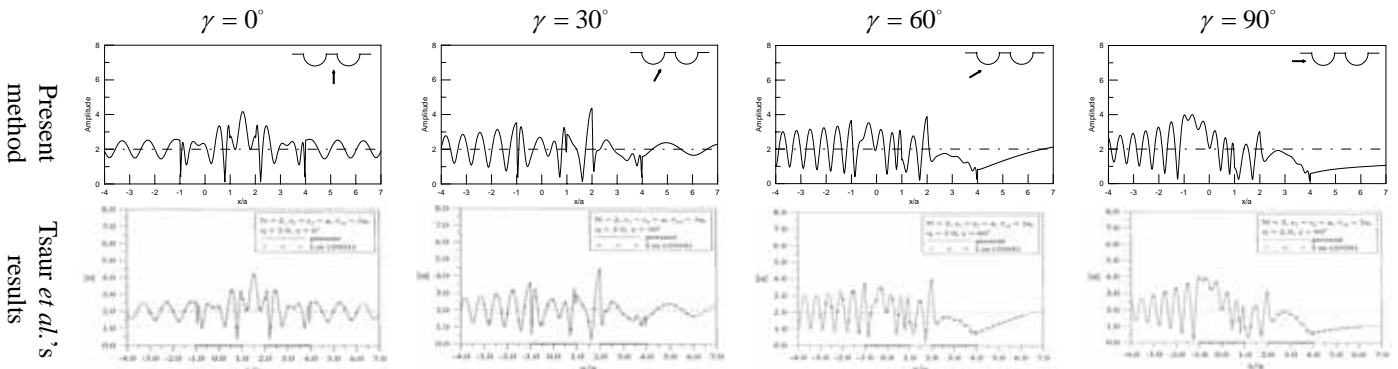


Figure 10 Limiting case of two canyons ($\mu^I / \mu^M = 10^{-8}$ and $\eta = 2$).

10. CONCLUSION

The first attempt to employ degenerate kernel in BIEM for problems with circular boundaries subject to the SH-wave was achieved. Not only canyon but also alluvial valley problems were treated. We have proposed a BIEM formulation by using degenerate kernels, null-field integral equation and Fourier series in companion with adaptive observer systems and vector decomposition. This method is a semi-analytical approach for problems with circular boundaries since only truncation error in the Fourier series is involved. Two limiting cases of inclusions, canyon and rigid footing, was also addressed. Good agreements are obtained after comparing with previous results. The surface motion of half-plane problem with alluvial valleys was determined. The analysis of amplification and interference effects for valley and inclusions subject to SH-waves may explain the ground motion either observed or recorded during earthquake. The method shows great generality and

$\mu^I / \mu^M = 10^{-8}$, the limiting case of successive canyons is obtained as shown in Figure 10. Tsauro *et al.* [15] and Fang [17] have both solved the problem of two semi-cylindrical alluvial valleys for the incident SH-wave. Tsauro *et al.* [15] pointed out that the deviation by Fang [17] is that Fang improperly used the orthogonal property. Good agreement is made after comparing with the results of Tsauro *et al.* [15]. For the incident angle of zero-degree, the surface displacement amplitude is symmetric. By increasing the incident angle, the displacement amplitude is gradually smaller in the back side of the alluvial valley or canyon due to the shield effect of two alluvial valleys or canyons. As the incident angle approaches ninety-degrees, the surface displacement amplitudes are all smaller than the “free field” in the back of the second alluvial. It indicates that two alluvial valleys can be the wave trap for the incident wave.

versatility for the problems with multiple circular cavities and inclusions of arbitrary radii and positions. Five advantages of singularity-free, no boundary-layer effect, well-posed model, exponential convergence and mesh-free approach are the main features of the proposed approach.

11. ACKNOWLEDGEMENT

The study is supported by the National Science Council of Taiwan, the Republic of China through the grant number NSC-95-2115-M-019-003-MY2.

12. REFERENCES

- [1] M.D. Trifunac, “Surface motion of a semi-cylindrical alluvial valley for incident plane SH waves”, *Bulletin the Seismological Society of America*, vol. 61(6), pp.1755-1770, 1971.
- [2] Y.H. Pao and C.C. Mow, “Diffraction of elastic waves and dynamics stress concentration”, *Crane*,

- New York, 1972.
- [3] M.D. Trifunac, "Scattering of plane SH waves by a semi-cylindrical canyon", *Earthquake Engineering and Structural Dynamics*, vol. 1, pp. 267-281, 1973.
- [4] V.W. Lee, M.D. Trifunac and A.M. ASCE, "Response of tunnels to incident SH-waves", *Journal of the Engineering Mechanics Division*, vol. 105 (EM4), pp. 643-659, 1978.
- [5] V.W. Lee, and M.E. Manoogian, "Surface motion above an arbitrary shape underground cavity for incident SH waves", *European Earthquake Engineering*, vol. 1, pp. 3-11, 1995.
- [6] M.E. Manoogian, "Scattering and diffraction of plane SH-waves by surface and subsurface discontinuities", Ph.D. Dissertation, *Department of Civil Engineering of University*, Southern California, USA, 1992.
- [7] M.E. Manoogian and V.W. Lee, "Diffraction of SH-waves by subsurface inclusions of arbitrary shape", *Journal of Engineering Mechanics*, vol. 122(2), pp. 123-129, 1996.
- [8] A. Rodriguez-Castellanos, F. Luzon and F.J. Sanchez-Sesma, "Diffraction of seismic waves in an elastic, cracked half plane using boundary integral formulation", *Soil Dynamics and Earthquake Engineering*, vol. 25, pp. 827-837, 2005.
- [9] P.Y. Chen, "Null-field integral equation approach for solving stress concentration problems with circular boundaries", Master thesis, *Department of Harbor and River Engineering, National Taiwan Ocean University*, Taiwan, 2006.
- [10] J.T. Chen, W.C. Shen and P.Y. Chen, "Analysis of circular torsion bar with circular holes using null-field approach", *Computer Modeling in Engineering Science*, Vol.12 (2), pp.109-119, 2006.
- [11] J.T. Chen and P.Y. Chen, "A semi-analytical approach for stress concentration of cantilever beams with circular holes under bending", *Journal of Mechanics*, Revised, 2006.
- [12] J.T. Chen, W.C. Shen and A.C. Wu, Null-field integral equations for stress field around circular holes under anti- plane shear, *Engineering Analysis with Boundary Elements*, Vol. 30, pp. 205-217, 2005.
- [13] J.T. Chen and H.-K. Hong, "Review of dual boundary element methods with emphasis on hypersingular integral and divergent series", *Applied Mechanics Reviews*, vol. 52, pp. 17-33, 1999.
- [14] J.T. Chen, L.W. Liu and H.-K. Hong, "Spurious and true eigensolutions of Helmholtz BIEs and BEMs for a multiply connected problem", *Proceedings of the Royal Society of London. Series A*, vol. 459, pp. 1891-1924, 2003.
- [15] D.H. Tsaor, K.H. Chang and J.G. Lin, "Response of multiple semi-circular cylindrical canyons subjected to plane SH-wave", *Asia Pacific Review of Engineering Science and Technology*, vol. 2(2), pp. 251-266, 2004.
- [16] V.W. Lee and M.E. Manoogian, "Surface motion above an arbitrary shape underground cavity for incident SH waves", *European Earthquake*

Engineering, vol. 1, pp. 3-11, 1995.

- [17] Y.G. Fang, "Scattering of plane SH-waves by multiple circular-arc valleys at the two-dimensional surface of the earth", *Earthquake Engineering and Engineering Vibration*, vol. 15(1), pp. 85-91, 1995.

半解析法求解多山谷沉積物入射SH波 之地表位移

陳柏源 陳正宗

國立台灣海洋大學河海工程學系

摘要

本文係使用零場積分方程搭配分離核函數與傅立葉級數求解含沉積山谷的外域赫姆茲問題。文中，利用退化核函數之特性，可解析求得當零場點直接佈在真實邊界上時的所有的奇異積分並免除主值計算的困擾。採用自適性觀察座標系統來充分掌握分離核函數的特性。本文中，半平面的問題使用映射法以及疊加的技巧來求解。透過零場積分方程推向邊界且均勻佈點，滿足邊界條件後可以得到一線性代數方程式，其中的未知傅立葉係數均可輕易地求得。由於誤差僅來自於擷取有限項的傅立葉級數，故本方法可視為“半解析法”。SH 坡入射沉積土或山谷的地震反應分析是本文探討的重點。在數值算例中，利用單個或連續沉積土以及特例的山谷與剛性夾雜問題來驗證此半解析法的正確性。本方法同時兼具五種優點：有良態模式、免於計算主值、無邊界曾效應以及不需佈網格的優點。

關鍵詞：分離核函數、傅立葉級數、零場積分方程、赫姆茲問題、SH 波、沉積山谷。